Current relaxation and mesoscopic fluctuations in disordered conductors

B. L. Al'tshuler, V. E. Kravtsov, and I. V. Lerner

B. P. Konstantinov Leningrad Institute of Nuclear Physics, Academy of Sciences of the USSR; Institute of Spectroscopy, Academy of Sciences of the USSR

(Submitted 28 July 1987)
Zh. Eksp. Teor. Fiz. **94**, 258–275 (April 1988)

Current relaxation in a disordered conductor is analyzed by an approach based on the nonlinear σ model. It is found that after a long time the relaxation current $j(t)$ is described by a log-normal asymptotic expression $j(t) \propto \exp[-(\ln^2 t)/u]$. The value of u increases without bound near the mobility threshold, with the result that relaxation processes are slowed dramatically. Mesoscopic fluctuations in the value of $j(t)$ are also considered. At absolute zero, $T = 0$, these fluctuations increase with time, so the mean value $\langle j(t) \rangle$ cannot be used to describe relaxation in specific samples. For $T \neq 0$ there is a broad interval of times in which the quantity $j(t)$ is self-averaging. In this interval, the log-normal asymptotic behavior of $\langle j(t) \rangle$ characterizes specific samples. It is also shown that in specific samples $j(t)$ contains reproducible aperiodic oscillations with a time scale $\hbar/T$ which reflect the distribution of impurities in the sample.

1. INTRODUCTION

The substantial progress toward an understanding of the properties of disordered metals which has been achieved in recent years has resulted from research on the quantum-mechanical corrections to the conductivity (see, for example, the reviews in Refs. 1 and 2). Even in the region of good metallic conductivity, where these corrections are small, they must be taken into consideration in an analysis of the behavior of the conductivity as a function of the temperature T, the magnetic field H, the dimensions L of the sample, and the frequency ω. In the present paper we show that the quantum-mechanical corrections determine the course of relaxation processes in disordered conductors. Incorporating these corrections is by no means a trivial matter. In a description of the relaxation after a long time, for example, it is not sufficient to consider the lowest-order perturbations. Furthermore, an ordinary renormalization-group analysis of localization theory is insufficient.[1-3]

As an example of a relaxation process we consider the time dependence of the electric current $\mathbf{j}$ when an external field $\mathbf{E}$ is turned on or off. For an arbitrary time dependence $\mathbf{E}(t)$, the current $\mathbf{j}(t)$ can be found if the frequency dependence of the conductivity, $\sigma(\omega)$, is known:

$$\mathbf{j}(t) = \int_0^\infty \mathbf{E}(t-t')\sigma(t')\,dt', \tag{1}$$

where $\sigma(t)$ is related to $\sigma(\omega)$ by the Fourier transformation

$$\sigma(t) = \int \sigma(\omega) e^{-i\omega t}\, d\omega/2\pi. \tag{2}$$

The quantity $\sigma(t)$ is the response of the system to an electric-field pulse which is a δ-function of the time.

When the quantum-mechanical corrections are ignored, the response function $\sigma(t)$ can be written

$$\sigma_0(t) = \frac{\sigma_0}{\tau} \exp\left(-\frac{t}{\tau}\right), \tag{3}$$

which corresponds to the ordinary Drude formula

$$\sigma(\omega) = \sigma_0(1 - i\omega\tau)^{-1}.$$

Here σ_0 is the residual conductivity, which is related to the one-spin state density ν and the classical value of the diffusion coefficient D_0 by the Einstein relation $\sigma_0 = 2e^2\nu D_0$, where $D_0 = l^2/d\tau$, l and τ are the mean free path and collision time of an electron, and d is the dimensionality of the space.

Expression (3) determines the response function only at early times, $t \lesssim \tau$. For $t > \tau$, the quantity $\sigma(t)$ is governed entirely by quantum-mechanical effects. The ordinary cooperon correction to $\sigma(\omega)$ is given by the expression[1,2]

$$\sigma_1(\omega) = -\frac{2e^2}{\pi\hbar} \int \frac{1}{q^2 - i\omega/D + L_{\varphi 0}^{-2}} \frac{d^d q}{(2\pi)^d}, \tag{4}$$

where $L_{\varphi 0} = (D_0 \tau_{\varphi 0})^{1/2}$ is the length scale over which the electron wave function undergoes phase relaxation due to inelastic processes, and $\tau_{\varphi 0}$ is the phase relaxation time. The component of $\sigma(t)$ corresponding to (4) is

$$\sigma_1(t) = -\frac{e^2}{2\pi^2\hbar} \frac{1}{t^{d/2}} (4\pi D_0)^{(2-d)/2} e^{-t/t_0}, \tag{5}$$

where we have $t_0 = \tau_{\varphi 0}$ for an isolated sample, and where we have

$$t_0 = \min\{\tau_{\varphi 0}, \hbar/E_c\} \tag{6}$$

for a cube of volume L^d with bulk contacts. Here $E_c = \hbar D/L^2$ is the width of the energy band which contains the exact one-electron levels which contribute to the conductivity.[4] This width is determined by the time L^2/D, which is the time required for an electron to diffuse to the contact, over which the phase relaxation occurs. According to (5), in the time interval $\tau < t < t_0$ the relaxation current thus falls off algebraically, while for $t > t_0$ the decay becomes exponential.

In Secs. 2 and 3 we show that the relaxation current is not described by the ordinary quantum-mechanical correction (4) after a long time. It turns out that in the limit $t \to \infty$ the decay of the relaxation current is far slower than the exponential decay (5), although it is faster than any power of t^{-1}:

$$\sigma_2(t) \propto \frac{\sigma}{\tau} \exp\left[-\frac{1}{4u} \ln^2 \frac{t}{\tau}\right]. \tag{7}$$

The value of u in (7) for a sample of any dimensionality d is

$$u = \ln(\sigma_0/\sigma). \tag{8}$$

 0038-5646/88/040795-10$04.00

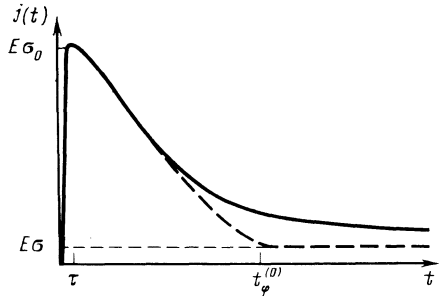

FIG. 1. Transient characteristics of a disordered conductor at low temperatures. At large values of u (i.e., at $\sigma_0/\sigma \gg 1$) the relaxation is greatly prolonged. The dashed line shows an exponential decay $j(t)$.

Here σ_0 and σ are respectively the bare value (the classical value) and the renormalized value (the observable value) of the static specific conductivity. An important point is that u can be extremely large (Sec. 3). In the three-dimensional case, for example, u increases without bound as the Anderson metal-insulator transition is approached. An increase in u causes all relaxation processes to slow down.

Figure 1 is a sketch of the transition characteristic, i.e., a plot of $j(t)$ for a discontinuous application of the field E. The current rises very rapidly (over a time on the order of τ) to its classical value $\mathbf{j}_0 = \sigma_0 \mathbf{E}$; $\mathbf{j}(t)$ then falls off, initially in accordance with the power law (5), and for $t \gg t_0$ in accordance with the log-normal law (7), to a steady-state value $\mathbf{j} = \sigma \mathbf{E}$ which is determined by the renormalized value of σ. As σ decreases (e.g., as the temperature is lowered, or as the order parameter changes, taking the sample closer to the Anderson transition), the quantity u increases in accordance with (8), stretching out the decay of the relaxation current. In this case the equilibrium regime is reached after an extremely long time.

The nonexponential decay of the response function (7) means that the disordered system cannot be characterized by one definite relaxation time. It is natural to associate with this system a set of relaxation times $\{t_\varphi\}$ with a distribution function $f(t_\varphi)$. It is in this form that we find an expression for $\sigma(t)$ (Sec. 3):

$$\sigma(t) \propto -\int \exp(-t/t_\varphi) f(t_\varphi)\, dt_\varphi / t_\varphi. \qquad (9)$$

The function $f(t_\varphi)$ falls off in a log-normal fashion at large t_φ. If it is assumed that in addition to the log-normal asymptotic behavior the function $f(t_\varphi)$ has a comparatively sharp maximum at $t_\varphi \sim t_0$ (Fig. 2), then expression (9) will describe the sum of quantum-mechanical components (5) and

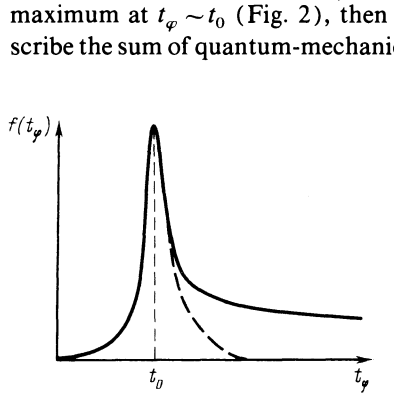

FIG. 2. Distribution of the phase relaxation times. At $t_\varphi > t_{\varphi 0}$, the distribution function (the solid line) falls off in log-normal fashion—far more slowly than exponentially (the dashed line).

(7). It is shown in Sec. 6 that the distribution function of the phase relaxation times is indeed of this nature in the electron-phonon interaction.

A distribution like $f(t_\varphi)$ has been found previously[5] for mesoscopic fluctuations in the static conductivity[6,7] and in the state density.[8] A distribution of this sort characterized the scatter in the values of these properties in an ensemble of samples having identical macroscopic characteristics. It has also been found[5] that under certain conditions the average values of quantities are inadequate for describing a specific sample. Here, on the other hand, we have only presented results for average values up to this point. Under what conditions is the average response function sufficient for describing relaxation processes in a specific sample? To answer this question we should calculate the variance of the mesoscopic fluctuations of $\sigma(t)$, i.e., the scatter in this quantity from sample to sample.

The fluctuations in $\sigma(t)$ are calculated in the formal limit $T = 0$ in Sec. 4. It turns out that for $t > t_0$ ($t_0 = \hbar/E_c$ at $T = 0$) these fluctuations exceed the mean value. This result means that expressions (3) and (7) for the response function, averaged over all realizations, do not describe the relaxation in a specific sample. The log-normal asymptotic behavior (7) is determined by the contribution of infrequent (improbable) realizations with large times t_φ.

This conclusion, however, is valid only at $T = 0$. When we take the thermal spreading of the Fermi distribution into account (Sec. 5; we ignore bulk inelastic processes), we find that reproducible aperiodic oscillations with a time scale of $\hbar/T$ appear in the response function. As is shown in Sec. 5, this situation has a certain ergodic aspect: Taking an average of $\sigma(t)$ over time intervals $\Delta t \gg \hbar/T$ is equivalent to taking an average over realizations. As a result, for the average of the response function over the interval Δt there exists a region of times (which depends on the value of Δt) in which the response function of a specific sample decays in accordance with the law (7).

The asymptotic response function remains log-normal when we take account of the phase relaxation of the electron wave function caused by an inelastic interaction in the volume. We demonstrate this point in Sec. 6 for the particular example of the electron-phonon interaction. The fluctuations in $\sigma(t)$, however, remain of a self-averaging nature over a wide time interval. As in the case $T = 0$, the relative magnitude of the fluctuations is proportional to $L^{-d/2}$. At $T = 0$ this small factor is offset by the circumstance that a nonalgebraic relaxation occurred at times $t \gtrsim \hbar/E_c = L^2/D$, which increase with the dimensions of the system. When inelastic processes are taken into account, the relaxation occurs over times $t \gtrsim \tau_{\varphi 0}$ which do not depend on L, so the fluctuations are suppressed in the thermodynamic limit. Over times

$$t \gtrsim (\tau_{\varphi 0}/4u) \ln(\tau_{\varphi 0}/\tau)$$

the relaxation processes in specific samples are characterized by the log-normal asymptotic expression (7).

2. QUANTUM-MECHANICAL CORRECTIONS TO THE FREQUENCY DEPENDENCE OF THE CONDUCTIVITY; ASYMPTOTIC BEHAVIOR OF THE RESPONSE FUNCTION

The behavior of the response function $\sigma(t)$ after a long time $t \gg t_0$ is determined by the frequency dependence of the

conductivity, $\sigma(\omega)$, at low frequencies, $\omega \ll t_0^{-1}$. A slow decay of the response function (7) evidently corresponds to an ω dependence of σ which has a singularity as $\omega \to 0$. In this section of the paper we discuss the reasons for the appearance of this singularity, which was first found in Ref. 9.

Under the condition $\omega t_0 < 1$, the frequency dependence of the conductivity can be sought as a power series in ω. In this section we approach the problem of the frequency dependence of the conductivity from the standpoint of an ordinary admixture diagram technique with separate diffusion and cooperon two-particle propagators.[10] In each specific diagram, both the electron Green's functions and the diffusion poles depend on ω. An expansion of the Green's function in the frequency leads to a series in $\omega\tau$, while an expansion of the diffusion or cooperon leads to a series in ωt_0. The frequency dependence of the conductivity can thus be written in the form $\sigma(\omega) = \sigma_1(\omega) + \sigma_2(\omega)$, where

$$\sigma_1(\omega) = \sigma_0 \sum C_n (i\omega\tau)^n, \tag{10}$$

$$\sigma_2(\omega) = \frac{e^2}{\hbar} \sum S_n (i\omega t_0)^n. \tag{11}$$

(There are also cross contributions, of course, but they will never be important, as we will see below.) In the classical limit we have $C_n = 1$ and $S_n = 0$, and sum (10) becomes the usual Drude formula, (3). When quantum-mechanical effects are taken into account, the coefficients C_n and S_n can be found as power series in a parameter, given in the two-dimensional case by

$$\alpha = (\hbar/2\varepsilon_F\tau)\ln(t_0/\tau). \tag{12}$$

[We are staying in the so-called leading-log approximation; i.e., we will ignore contributions proportional to $(\hbar/\varepsilon_F\tau)^n \ln^m (t_0/\tau)$ with $n > m$.]

We wish to stress that perturbation theory in higher orders in α leads to nonvanishing contributions to the frequency dependence $\sigma(\omega)$. We know quite well that the quantum-mechanical correction (4) to the static conductivity, although it appears to be the result of a first-order perturbation theory in α, actually describes the sum of all of the quantum-mechanical contributions. With $d = 2$, all of the leading-log contributions (like the corresponding contributions with $d \neq 2$, which are not analytic in τ/t_0) cancel out in all orders of perturbation theory other than the first. This cancellation follows from the renormalizability of the nonlinear σ model: an effective field theory for the localization problem which was proposed by Wegner[11] and which has been studied by several investigators.[12-16] At a finite frequency ω, on the other hand, this cancellation does not occur.

We are considering only the case $L \gg l$, i.e., $t_0 \gg \tau$. At first glance it would appear that we could ignore the contribution of (10) to $\sigma(\omega)$. Actually, the long-time asymptotic behavior of the response function), (7), is governed specifically by this contribution. The reason lies in the very rapid growth of the coefficients in expansion (10) with increasing n. In the following section of this paper we show that the coefficients C_n increase more rapidly than $n!$:

$$C_n \propto \exp[u(n^2+2n)]. \tag{13}$$

This growth leads to a singularity in $\sigma(\omega)$ as $\omega \to 0$. The coefficients S_n in expansion (11), on the other hand, grow far more slowly, and their contribution to the relaxation current falls off far more rapidly than (7).

To verify that expressions (10) and (13) for $\sigma(\omega)$ are equivalent to the long-time asymptotic behavior in (7) of response function $\sigma(t)$, it is sufficient to substitute (7) into the relation

$$\sigma(\omega) = \int e^{i\omega t}\sigma(t)\,dt$$

and to expand the exponential function in a series. An evaluation of the integrals at each power ω^n leads to relation (13).

A growth law similar to (13) has been observed in a study of the various components of the frequency dependence of the diffusion coefficient in an analysis of the stability of single-parameter scaling in localization theory.[9] Even earlier, it had been shown that a dependence of the type (13) arises in a study of the higher-order moments of the local state density (the participation ratios).[17] Finally, a similar growth law is characteristic of the higher-order moments of mesoscopic fluctuations in the conductivity and the total state density.[5]

All of the results have been derived in a certain generalization of the nonlinear σ model. In the following section of this paper we offer a derivation of relation (13) in this formalism. At this point we will attempt to clarify the reason for this rapid growth of the coefficients C_n in terms of an admixture diagram technique. Figure 3a shows a diagram for calculating the coefficients C_n in the classical limit (in zeroth order in α). This diagram is a simple electron loop, in which only the upper Green's function depends on ω; the vertices with arrows arise from the differentiation[1)] of the Green's function with respect to ω. We see that the entire n dependence of this diagram arises from the factor $\zeta_{0,n} \propto (-i\tau)^{n+1}$, and as a result we find the Drude formula. Here

$$\zeta_{m,n} = \int G_R^{m+1}(\mathbf{p})\, G_A^{n+1}(\mathbf{p})\, \frac{d^d p}{(2\pi)^d}$$

$$= 2\pi\nu i(-i\tau)^{m+n+1} \frac{(m+n)!\,(-1)^n}{m!\,n!},$$

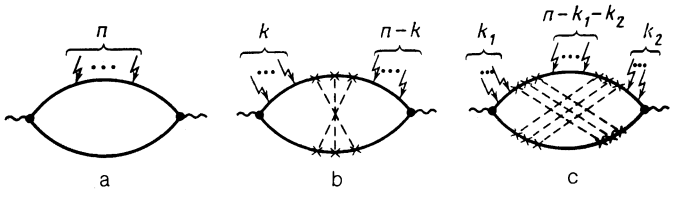

FIG. 3. Examples of diagrams which contribute to the expansion of the coefficient C_n in powers of the semiclassical parameter α. Solid lines—electron Green's functions; arrows—differentiation with respect to the frequency; dashed lines—averaging over admixtures.

where $G_{R(A)}(\mathbf{p})$ is the retarded (or advanced) Green's function of an electron in the momentum representation. The first-order perturbation theory in parameter (12) is determined by diagrams of the type in Fig. 3b. Each of these diagrams is proportional to $\zeta_{1,n+1} \propto (n+1)$. The number of diagrams of the same type is also equal to $n+1$: the number of distributions of n differentiations with respect to the two Green's functions. Accordingly, the contribution to C_n which is linear in α is proportional to $n^2\alpha$. As we move on to second order in α, we find that the number of diagrams which contribute to C_n increases to n^2, and each contains a factor $\zeta_{2,n+2} \propto n^2$. In other words, this component is proportional to $n^4\alpha^2$. In calculating C_n we thus find a series in $n^2\alpha$ instead of a series in α, such as arises in the calculation of the static conductivity. The meaning is that for any arbitrarily small value of α one can find a value of n at which it is not legitimate to restrict the analysis to the lowest-order perturbation theory, and the entire diagram series must be summed.

Attempts to carry out this summation by the admixture diagram technique or even to estimate the contributions of higher orders in α run into insurmountable difficulties because the diagrams contain, in addition to the diffusions and cooperons, some additional admixture lines,[10] various numbers of diffusion poles in the diagrams of a given perturbation-theory order, etc. It is vastly more productive, as we know quite well, to work in a formalism based on the nonlinear σ model. An analysis based on the formalism is described in the following section of this paper. It leads to the growth law (13) for the coefficients C_n and thus asymptotic behavior (7). The results of the analysis in Sec. 3 were published previously in a brief communication.[18]

3. EXPANDED NONLINEAR σ MODEL

The nonlinear σ model is ordinarily used in localization theory to calculate the correlation function for the densities of noninteracting electrons in a random potential.[13,14] This correlation function is used to reconstruct a normalized diffusion coefficient, which is related to the conductivity by the Einstein equation. Methods for calculating the conductivity σ directly were developed in Refs. 19–21 and 5. To calculate the frequency dependence $\sigma(\omega)$ here, we modify the formalism of Ref. 19, which was generalized in Ref. 5 in a calculation of the moments of mesoscopic fluctuations.

The conductivity of a cube of volume L^d can be written in the form[2)]

$$\sigma_{\alpha\beta} = -\frac{e^2}{16\pi N^2 L^d}\left\{\int \mathcal{D}Q e^{-F}\right\}^{-1} \times \int \mathcal{D}Q \,\mathrm{tr}\left\{\frac{\partial^2}{\partial A_\alpha\, \partial A_\beta} e^{-F}\right\}\Big|_{\substack{N=0\\ A=0}}. \tag{14}$$

In zeroth order in $\omega\tau$, the functional of the nonlinear σ model in the external field of a source A has the natural form

$$F = \frac{\pi\nu D}{8}\int \mathrm{tr}(\nabla_\alpha Q)^2\, d^dr \tag{15a}$$

$$+\frac{i\pi\nu\omega}{4}\int \mathrm{tr}(\Lambda Q)\, d^dr. \tag{15b}$$

Here, however, ∇_α is a covariant derivative, which differs from the gradient ∂_α by the commutator

$$\nabla_\alpha Q \equiv \partial_\alpha Q - i[A_\alpha, Q]. \tag{16}$$

In Eqs. (14)–(16), α and β are vector indices in a d-dimensional space, and $Q(\mathbf{r})$ and $\mathbf{A}(\mathbf{r})$ are Hermitian matrix quaternion fields with the structure

$$\begin{aligned} &Q = Q^\mu \tau_\mu, \quad Q^\mu = Q_{ab}^{pp',\mu}, \quad (Q^\mu)^* = Q^\mu, \\ &\mathbf{A} = \mathbf{A}^\mu \tau_\mu, \quad \mathbf{A}^\mu = A_{ab}^{pp',\mu}; \quad (\mathbf{A}^\mu)^* = -\mathbf{A}^\mu. \end{aligned} \tag{17}$$

Here the τ_μ are unit quaternions: $\tau_0 = I$, and $\tau_{1,2,3} = i\hat{\sigma}_{x,y,z}$ ($\hat{\sigma}$ are the Pauli matrices. The replica indices a and b run over values from 1 to N; in the final results, N should be set equal to zero. The indices p and p' each take on two values, and the matrix Λ in (15), which is diagonal in these indices and which is given by

$$\Lambda = (\sigma_z)^{pp'} \otimes \delta_{ab} \otimes \tau_0, \tag{18}$$

reflects the presence of retarded and advanced Green's functions in the original microscopic expression for the conductivity. The functional (15) is nonlinear because of geometric limitations imposed on the field Q:

$$Q^2 = I, \quad \mathrm{tr}\, Q = 0. \tag{19}$$

Expressions (14) and (15) were derived (in a slightly different notation) in Refs. 19 and 5 from the Kubo formula for the conductivity of noninteracting electrons in a random potential. In those earlier studies, the simplest expression for A, with

$$\mathbf{A}^{pp,\mu} = 0, \quad \mathbf{A}^{pp',1} = \mathbf{A}^{pp',2} = 0,$$

was used in order to find the correct coefficient of the exponential function in (14). These limitations are not mandatory because of the gauge invariance of functional (15) under the transformations

$$Q \to U^+ Q U, \quad A_\alpha \to U^+ A_\alpha U - i(\partial_\alpha U) U^+, \tag{20}$$

where $U(\mathbf{r})$ is a unitary quaternion-real matrix: i.e., $U \in \mathrm{Sp}(2N)$, where $\mathrm{Sp}(N)$ is the simplectic group. [Conditions (17) and (19) means that Q belongs to a quaternion Grassmann manifold $\mathrm{Sp}(2N)/\mathrm{Sp}(N) \otimes \mathrm{Sp}(N)$.]

In this section of the paper we are interested in the case $T = 0$ and frequencies which are so low,

$$\omega \ll E_c, \tag{21}$$

that the infrared catastrophes are cut off by the quantity $E_c = /D/L^2$, i.e., by the finite dimensions of the system. A renormalization-group analysis of the functional (15) is carried out in the usual way[13,9]: The field Q is represented as the product $Q(\mathbf{r}) = \tilde{U}^+(\mathbf{r}) Q_0(\mathbf{r}) \tilde{U}(\mathbf{r})$, where $Q_0(\mathbf{r})$ are the fast components, and $\tilde{Q}(\mathbf{r}) \equiv \tilde{U}^+(\mathbf{r}) \Lambda \tilde{U}(\mathbf{r})$ the slow components, of the field $Q(\mathbf{r})$. A renormalized functional is found by integrating over Q_0,

$$\tilde{F} = -\ln \int \mathcal{D}Q_0 \exp[-F], \tag{22}$$

and depends only on $\tilde{Q}$. By virtue of the gauge invariance of (20), the charge in $\mathrm{tr}(\nabla Q)^2$ in (15a) is renormalized in the same way as the charge in $\mathrm{tr}(\partial Q)^2$ in the ordinary σ model. (This assertion was verified by direct calculations in Ref. 19.) A renormalized (i.e., physical) value of the conductivity is calculated with the help of (14). It of course turns out to be proportional to the renormalized value of the coeffi-

cient of $\mathrm{tr}(\nabla Q)^2$ in (15). We know quite well[12-16] that the renormalized value found for the static conductivity in this way obeys the Gell-Mann–Low equation, which is written in the single-loop approximation as

$$\frac{dg}{d\ln(L/l)} = \varepsilon g - 1, \tag{23}$$

where $\varepsilon = d-2$, and g is the dimensional conductance of a cube of volume L^d, given by

$$g \equiv \frac{\hbar\sigma}{e^2} L^{\varepsilon}\alpha_d, \quad \alpha_d = \begin{cases} \pi, & d=1 \\ \pi^2, & d=2. \\ 2\pi^2, & d=3 \end{cases} \tag{24}$$

It is convenient to write the solution of Eq. (23) in the form

$$g = g_c + (g_0 - g_c)(L/l)^{\varepsilon}, \tag{25}$$

where $g_0 = g(L=l) \sim (\varepsilon_F \tau)^{d-1} \gg 1$ is the bare value of the conductance, equal to the classical conductance of a cube of volume l^d, and $g_c = \varepsilon^{-1}$ with $\varepsilon > 0$ means the critical value of the conductance. The conductivity σ given by expressions (24), (25) agrees with the conductivity calculated from the perturbation expression (4). This agreement reflects the cancellation of the contributions from higher-order perturbation theories.[10,15]

Vertex (15b) is not renormalized by virtue of the conservation of the number of particles.[12-14] The frequency dependence of the conductivity determined by this vertex can be found by perturbation theory from (14). A perturbation technique within the framework of the nonlinear σ model is described in several places,[13,15,5] and we will not reproduce the corresponding calculations here. We would like to point out that the integrals over the momenta which diverge at the lower limit are cut off under condition (21) by the reciprocal dimension of the system. The result is an expansion in ω/E_c, (11) (at $T=0$ we have $t_0 = E_c^{-1}$). The expansion coefficients do not contain combinatorial factors growing faster than $n!$.

When only functional (15) is taken into account, no corrections to the conductivity which contain powers of $\omega\tau$ arise. An effective field-theory functional was derived in Ref. 9 for calculating the density correlation function with these corrections. In the derivation of that functional from the Schrödinger equation for a particle in a random potential, some additional contributions arise, consisting of all possible products of $\omega\tau\Lambda Q$ and $l\partial_\alpha Q$. Similar vertices arise in a functional which makes it possible to calculate the conductivity directly. A very important point is that the gauge variance which we mentioned above remains in force for the functional augmented in this manner. It depends only on the covariant derivatives ∇_α in (16).

To calculate the observable value of $\sigma(\omega)$, we should renormalize all the additional vertices and then, incorporating them in the functional F, calculate a path integral in the zeroth approximation in g^{-1}, i.e., by setting $Q=\Lambda$ [see (18)]. In the renormalization-group procedure, only the vertices which do not vanish in the case $Q=\Lambda$ contribute to the frequency dependence of conductivity (10). A functional which contains these vertices can be written in the form[3)]

$$F = \sum_n F_2^n,$$

$$F_2^n = \sum_n (\omega\tau)^n \sum_{\mathscr{P}} Z_2^n(\mathscr{P}) \int \mathrm{tr}\{\mathscr{P}(\nabla_\alpha Q)^2 (\Lambda Q)^n\} d^d r. \tag{26}$$

The superscript and subscript on F_m^n specify the powers of $\omega\Lambda Q$ and $\partial_\alpha Q$, respectively. The symbol $\mathscr{P}$ means all possible permutations of the noncommitting matrices in the tr. The seed values of the coefficients Z_m^n are generally different for different permutations.

In the zeroth approximation ($Q=\Lambda$) we have $\partial_\alpha Q = 0$, so the result of the path integration in (14) is proportional to $\mathrm{tr}\,\mathbf{A}^2$. Differentiation with respect to the source $\mathbf{A}$ leads to expression (10), with

$$C_n \propto \sum_{\mathscr{P}} Z_2^n(\mathscr{P}).$$

Consequently, $\sigma(\omega)$ is determined by the behavior of the charges Z_2^n under the renormalization-group transformations.

Although only vertices (26) contributed directly to (10), we need to also consider some additional vertices which contain a large number of covariant derivatives. The situation is that these are the vertices which (as we will show below) determine the renormalization of the charges Z_2^n of functional (26) under renormalization-group transformations. Nevertheless, we will first discuss the situation which arises if we ignore the contributions of higher order in $\nabla_\alpha Q$ and restrict the analysis to the functional (26). Most of the qualitative features of the phenomenon remain the same.

In Ref. 9, where vertices F_m^n with $m>2$ were ignored, a renormalization-group equation was derived for the charge Z_2^n, which can be written in the single-loop approximation in the following symbolic form[4)]:

$$\frac{dZ_2^n}{d\ln(L/l)} = g^{-1}(n^2-n)Z_2^n. \tag{27}$$

A rigorous derivation of the corresponding renormalization-group equations for the charges was carried out in Refs. 5 and 6 with gradient-free vertices $F_0^n \propto \mathrm{tr}(\Lambda Q)^n$. We will accordingly omit the essentially similar derivation of Eq. (27). The solution of this equation is

$$Z_2^n \propto \exp(E_2^n u). \tag{28}$$

Here $E_2^n = n^2 - n$ and the quantity u is found from (23)–(25):

$$u = \int \frac{d\ln(L/l)}{g(L)} = \ln\left(\frac{g-g_c}{g_0-g_c}\frac{g_0}{g}\right) = \ln\frac{\sigma_0}{\sigma}. \tag{29}$$

In the weak-localization region, this quantity is small: $u \sim g_0^{-1}\ln(L/l)$ with $d=2$. An important point is that as an insulating state is approached the quantity u becomes large even in the range of applicability of the single-loop (leading-log) approximation. At the boundary of this region we have

$$u = \begin{cases} \ln g_0, & d=2 \\ \ln(1-g_c/g_0)^{-1}, & g_0 \to g_c, \quad d=2+\varepsilon \end{cases}. \tag{30}$$

Expressions (28)–(30) describe the growth of the charges Z_2^n with increasing n. Near the metal-insulator transition these charges have a critical power-law dependence with an exponent $-E_2^n$:

$$Z_2^n \propto (g_0 - g_c)^{-E_2^n}.$$

We can write a description of how the other additional

vertices influence charge renormalization (26). It can be shown that a series of vertices of the type

$$F_k^n=(\omega\tau)^n Z_{2k}^n(\mathscr{P})\int \mathrm{tr}\,\mathscr{P}\{\nabla_{\alpha_1}Q\dots\nabla_{\alpha_{2k}}Q(\Lambda Q)^n\}d^dr\hat{\varepsilon}_{\alpha_1\dots\alpha_{2k}} \tag{31}$$

appears in the derivation of an effective field theory from an original microscopic model of free electrons in a random potential. Here $\hat{\varepsilon}_{\alpha_1\dots\alpha_{2k}}$ is the absolutely symmetric tensor, and the bare values are

$$Z_{2k}^n(L=l)\sim l^{2k-2-\varepsilon}g_0.$$

The most important vertices are

$$F_k^0=Z_{2k}^0\int \mathrm{tr}\{\nabla_{\alpha_1}Q\dots\nabla_{\alpha_{2k}}Q\}d^dr\hat{\varepsilon}_{\alpha_1\dots\alpha_{2k}}. \tag{32}$$

Vertices of this sort are not ordinarily taken into consideration, since the normal dimensionality of the charges Z_{2k}^0 is $d-2k$; i.e., for $k>d/2$ they are formally negligible. Their anomalous dimensionality, however, turns out to be extremely large. It is found that at $d=2$ these charges increase in accordance with the following law under renormalization-group transformations:

$$Z_{2k}^0\propto\exp[(k^2-k)u]. \tag{33}$$

A proof of this law is given by Kravtsov, Lerner, and Yudson.[26]

Let us demonstrate how the vertices (32) influence the renormalization of charges Z_2^n in (26), which contribute directly to the conductivity. We first note that if we substitute expression (16) for the covariant derivative into (32) we find a set of vertices which contain various powers of the gradients ∂_α and of the sources A_α. The only vertices which can contribute to charge renormalization (26) [and to conductivity (14)] are those in which the power of A is no greater than two. In a description of the effect of the vertices (32) on the renormalization of observable quantities, we should therefore retain in (32) the two gauge derivatives ∇_α, replacing the others by ordinary gradients ∂_α. The gauge invariance makes it possible, however, to retain in (32) only the gradients, i.e., to carry out all the calculations under the condition $\mathbf{A}=0$ and to wait until the final expression to make the substitution $(\partial_\alpha)^2\to(\nabla_\alpha)^1$.

Let us examine the single-loop contribution to the renormalization-group transformation (22), which is proportional to the product of vertices F_{2n+2}^0 and F_0^1 [see (15b)]. The corresponding diagram is shown in Fig. 4. Each line in this diagram is a diffusion propagator $(Dq^2)^{-1}$; an integration is carried out over the momentum q (where $\lambda l^{-1}<q<l^{-1}$, and λ is a scaling factor). This diagram is accordingly logarithmic in the case $d=2$ if we single out in vertex F_{2n+2}^0 the two gradients from the "fast" components of the field Q (the effect is to give rise to a factor of q^2 in the momentum representation), and if we take the other $2n$ gradients from the "slow" components. Consequently, the calculations reveal a vertex[5] which contains $2n$ gradients and a field ΛQ, i.e., the vertex F_{2n}^1. When the contribution of this diagram and the definition of u in (29) are taken into account, we can write the renormalization-group equations for the charge Z_{2n}^1 in the following symbolic form[4]:

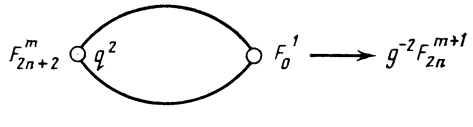

FIG. 4. Single-loop contribution of a vortex containing $2n+2$ gradients to the renormalization-group transformation of a vertex containing $2n$ gradients.

$$\frac{dZ_{2n}^1}{du}=E_{2n}^1Z_{2n}^1+g^{-1}Z_{2n+2}^1, \tag{34}$$

where E_{2n}^1 is the highest eigenvalue which arises during the renormalization of F_{2n}^1 if the other vertices are ignored. The growth index in the inhomogeneous term in Eq. (31) is, by virtue of the factor $g^{-1}\propto e^u$, one larger than the growth index in Z_{2n+2}^0, which is n^2+n, according to (32). It turns out to be greater than E_{2n}^1, so the u dependence of the charges Z_{2n}^1 is not the intrinsic dependence but that imposed by the solution of Eq. (34).

In renormalization-group transformations, the vertices with a large number of gradients thus influence the renormalization of the vertices in which the number of $\partial_\alpha Q$ decreases, but powers of ΛQ arise. On the other hand, there is an inverse effect. Consequently, the renormalization-group equations have a triangular structure. In each step (as shown in Fig. 4), the number of gradients is reduced by two, while the number of matrices ΛQ is increased by one. The sequential decrease in the number of gradients and the growth in the power in the renormalization-group transformations can be described by

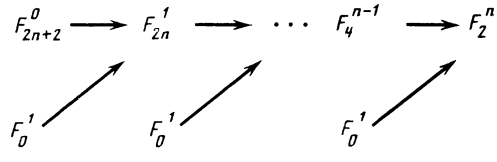

(35)

The growth index of the vertex $F_{2(n-k)}^{k+1}$ increases by one in each step of the transformations (35), since the structure of the renormalization-group equation is analogous to that of (34) in each step. As a result we find

$$E_2^n=n^2+2n. \tag{36}$$

This result proves expressions (11) and (13) for the frequency dependence of the conductivity, $\sigma(\omega)$. To make the transformation to $\sigma(t)$, it is convenient to use the identity

$$\exp(un^2)=\frac{1}{(4\pi u)^{1/2}}\int_0^\infty\left(\frac{t_\varphi}{\tau}\right)^n\exp\left[-\frac{1}{4u}\ln^2\frac{t_\varphi}{\tau}\right]\frac{dt_\varphi}{t_\varphi}. \tag{37}$$

As will become clear below, it is not by chance that we have designated the integration variable t_φ. Substituting expression (13) for the coefficients C_n into (10), using identity (37), and switching the order of the summation and the integration (an approach similar to Borel summation of asymptotic series) we find

$$\sigma(t)\propto-\frac{\sigma_0}{\tau}\int_0^\infty e^{-t/t_\varphi}\exp\left[-\frac{1}{4u}\ln^2\frac{t_\varphi}{\tau}\right]\frac{dt_\varphi}{t_\varphi}. \tag{38}$$

After an integration over t_φ, this result leads to a log-normal

asymptotic expression for the response function (7). Expression (38) is of independent interest, however. We see that the nonexponential decay of the response function (7) is found as the result of averaging exponential contributions $\exp(-t/t_\varphi)$ with a relaxation-time distribution which has a log-normal asymptotic behavior at long relaxation times t_φ. If we assume that this distribution function has a comparatively sharp maximum at $t_\varphi \approx t_0$, we find expression (8), which describes both the asymptotic response function (7) and the ordinary exponential contribution to $\sigma(t)$, (5). (In Sec. 6 we demonstrate how this form of the t_φ distribution function is found as a result of a direct calculation.) We thus see that the prolonged relaxation is determined by the wide scatter in the times t_φ. In the following section of this paper we will discuss whether this scatter is a property of a specific conductor or whether it is a mesoscopic scatter from sample to sample.

4. MESOSCOPIC FLUCTUATIONS IN THE RESPONSE FUNCTION

At zero temperature, a sample of any dimension L is mesoscopic. This statement means that such characteristics of the sample as its conductivity and state density are not self-averaging for $d \leqslant 2$; i.e., their relative scatter from sample to sample does not decrease with increasing L. For $2 < d < 4$, this scatter is also anomalously large: The relative magnitude of the fluctuations falls off as L^{2-d} (Refs. 6 and 7), not as $L^{-d/2}$, with increasing L.

A question which naturally arises is whether the mesoscopic fluctuations of the response $G(t)$ are large. In other words, does the nonexponential decay of this function at long times described by (7) characterize processes in an individual sample, or is it a consequence of a formal average over an entire ensemble of samples? To answer this question, we calculate the fluctuation moments of $\sigma(t)$, which completely characterize the scatter in this value from sample to sample:

$$K(t_1,\ldots,t_k) \equiv \left\langle \prod_{j=1}^{k} \sigma(t_j) \right\rangle_c = \left\langle \prod_{j=1}^{k} \int \frac{d\omega_j}{2\pi} \sigma(\omega_j) e^{-i\omega_j t_j} \right\rangle_c, \tag{39}$$

where the angle brackets mean an average over realizations of the random potential (i.e., over the ensemble of samples), and $\langle \ldots \rangle_c$ represents irreducible averages (cumulants).

Mesoscopic averages of the type (39) can be determined by generalizing the technique developed in the preceding section of the paper in a natural way. A formalism for calculating mesoscopic fluctuations of the static conductivity on the basis of an effective-field theory was developed in Ref. 5. Analogously, we can derive the following expression for the moments of the mesoscopic fluctuations in $\sigma(\omega)$:

$$K(\omega_1,\ldots,\omega_k) \equiv \left\langle \prod_{j=1}^{k} \sigma(\omega_j) \right\rangle_c$$

$$= \left(\frac{-e^2}{16\pi N^2 L^d}\right)^k \int \mathcal{D}Q \prod_{j=1}^{k} \operatorname{tr} \frac{\partial^2}{\partial A_j^2} e^{-\mathcal{F}} \left\{ \int \mathcal{D}Q e^{-\mathcal{F}} \right\}^{-1} \Big|_{\substack{N=0 \\ A=0}}. \tag{40}$$

The functional $\mathcal{F}$ is found from that described in the preceding section [see (15), (31)], through the assignment of an additional pair of indices i, j to all the matrix fields and through the replacement of the matrix $\omega\Lambda$ in (15b) and (31) by the following matrix, which is diagonal in i, j:

$$\begin{pmatrix} \omega_1 & & \\ & \ddots & \\ & & \omega_k \end{pmatrix}_{ij} \otimes \Lambda. \tag{41}$$

The additional indices are introduced in order to distinguish the variables referring to various conductivities in the product in (40). In the original formulation of the theory at the microscopic level, these indices specified the various current loops which describe the conductivity of a given sample (before an average is taken over impurities).[5] The introduction of additional indices makes it possible to avoid nonphysical diagrams which do not decay into k current loops before the averaging (such diagrams, which contain loops with more than two external lines, unavoidably arise in an effective field theory). The field of the source A is diagonal in i, j in this case ($A_{ij} \equiv A_i \delta_{ij}$), and the structure of the derivatives in (40) causes the nonphysical diagrams to vanish.

The vertices $\mathcal{F}^n_k$, which are found from the vertices (31) by the procedure described above for transforming from F to $\mathcal{F}$, contribute directly to (40). After calculations similar to those carried out in the preceding section, we find

$$K(\omega_1,\ldots,\omega_k) = \left(\frac{e^2}{\hbar}\frac{l^2}{L^d}\right)^{k-1} \sigma_0 \sum_{n}^{k-1} \sum_{n_1+\ldots+n_k=n} (i\omega_1\tau)^{n_1} \ldots (i\omega_k\tau)^{n_k} C^n_{\{k\}}, \tag{42}$$

where the coefficients $C^n_{\{k\}}$ are proportional to the renormalized charges Z^n_{2k} for the vertices of the form (31), and the summation is carried out over all possible partitions $\{k\}$ of the number n into a sum of k natural numbers. The coefficients $C^n_{\{k\}}$ depend relatively weakly on the partition $\{k\}$. The dependence of $C^n_{\{k\}}$ on n and k is determined primarily by the exceedingly rapid growth of the charges Z^n_{2k}. As above, we find that the growth index of these charges is determined by the influence of vertices of the $\mathcal{F}^0_{2(n+k)}$ type, in a diagram similar to (35). As a result we find

$$C^n_{\{k\}} \infty Z_{2k}{}^n \propto \exp\{u[(n+k)^2 - k]\}. \tag{43}$$

Substituting (43) into (42) and then into (39), and using the identity (37) to sum this series, we find the following result for the k th fluctuation moment $K(t_1,\ldots,t_k)$:

$$K(t_1,\ldots,t_k) \sim \left(\frac{e^2}{\hbar} L^{2-d}\right)^k \frac{g}{t_0^{k-1}\tau} \int_0^\infty e^{-t_s/t_\varphi} \exp\left[-\frac{1}{4u}\ln^2\frac{t_\varphi}{\tau}\right] \frac{dt_\varphi}{t_\varphi}. \tag{44}$$

The time dependence of this expression differs from that in (38), for the average response function $\langle\sigma(t)\rangle$, one by the replacement $t \to t_s \equiv t_1 + \ldots + t_k$. We thus find

$$K(t_1,\ldots,t_k) \sim \left(\frac{e^2}{\hbar} L^{2-d}\right)^k \frac{g}{t_0^{k-1}\tau} \exp\left[-\frac{1}{4u}\ln^2\frac{t_s}{\tau}\right]. \tag{45}$$

Comparison of this expression with (7) shows that the k th moment falls off considerably more slowly than $\langle\sigma(t)\rangle^k$ over time. This result means that after a long time, when $\langle\sigma(t)\rangle$ is described by expression (7), the scatter in the val-

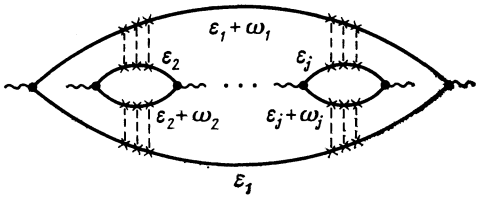

FIG. 5. Diagrams which dominate $\langle\sigma(t_1)\ldots\sigma(t_k)\rangle_c$ at times which are not too large.

ues of $\sigma(t)$ from sample to sample will be very large. Consequently, the average value of $\sigma(t)$ is not representative of a specific sample.

Let us find the scatter in the values of $\sigma(t)$ at times for which the average value $\langle\sigma(t)\rangle$ is described by (5). [In the metallic region, where the value of u in (7) is small, the range of applicability of expression (5) also extends to times greater than t_0.] In this region, the magnitude of the mesoscopic fluctuations can be found easily by ordinary perturbation theory. The k th irreducible fluctuation moment is determined primarily by diagrams of the type shown in Fig. 5. Calculations yield

$$K(t_1,\ldots,t_k)\sim\left(\frac{e^2}{\hbar}L^{2-d}\right)^k\frac{1}{t_s^k}\left(\frac{t_s}{t_0}\right)^{(2-d/2)(k-1)}g^{2-k}e^{-t_s/t_0}, \tag{46}$$

where $t_s=t_1+\ldots+t_k$. In particular, the relative variance of the response function in the case $t_1=t_2=t$ is

$$\frac{\langle\delta\sigma^2(t)\rangle}{\langle\sigma(t)\rangle^2}=\left(\frac{t}{t_0}\right)^{d/2}=\frac{(Dt)^{d/2}}{L^d}. \tag{47}$$

The mesoscopic fluctuations in the value of $\sigma(t)$, while small for $t<t_0$, become substantial for $t>t_0$ [this assertion applies only to the case $T=0$, in which the vortex t_0 in (4) is equal to L^2/D], and they are particularly large with respect to the average value at $t>(t_0/4u)\ln(t_0/\tau)$, i.e., in the region of applicability of asymptotic expressions (7) and (45).

We wish to stress that the relative variance of $\sigma(t)$ falls off as L^{-d} as the sample dimensions increase. Nevertheless, for the times of interest here, $t>t_0$, where relaxation processes are important, fluctuations are large even in the limit $L\to\infty$. The explanation is that at $T=0$ relaxation processes occur only in the bulk contacts at the boundary of the sample. The relaxation time $t_0=L^2/D$ increases with increasing dimensions, so when we take the thermodynamic limit $L\to\infty$ the times of interest also tend toward infinity.

Even at extremely low temperatures, however, the phase relaxation time of the electron wave function ($\tau_{\varphi 0}$), corresponding to relaxation due to inelastic interactions in the volume, becomes shorter than L^2/D. As we will see in Sec. 6, the average response function $\langle\sigma(t)\rangle$ is characterized again in this situation by a log-normal asymptotic behavior, which is reached at times $\tau_{\varphi 0}\ll t\ll L^2/D$. However, the factor L^{-d} in the variances has the consequence that at fixed time t satisfying this inequality the fluctuations $\sigma(t)$ are inconsequential in the thermodynamic limit. For samples of comparatively small dimensions ($L\lesssim(\hbar D/T)^{1/2}$, $(D\tau_{\varphi 0})^{1/2}$), on the other hand, the fluctuations remain large. In the following section of this paper we show that their statistics, however, are qualitatively different from those in the case $T=0$.

5. FLUCTUATIONS IN $\sigma(t)$ AT NONZERO TEMPERATURES

In this section we analyze the effect of nonzero temperatures on the fluctuations in the response function. For the moment, we ignore the phase relaxation caused by inelastic interactions in the sample; i.e., we assume as before that the relaxation occurs exclusively at the boundary of the sample. In this approximation, the temperature affects only the fluctuations, without affecting the average values. We will show that incorporating the temperature leads not only to a decrease in the fluctuations at $T>E_c$, as in the static case,[8] but also to "mesoscopic grass" in the response function: reproducible aperiodic fluctuations in $\sigma(t)$ with a time scale $\delta t\sim\hbar/T$.

At $T\neq 0$, the Fourier transform of the variance $\langle\sigma(t_1)\sigma(t_2)\rangle_c$ is

$$K_T(\omega_1,\omega_2)=\int_{-\infty}^{\infty}d\varepsilon_1\int_{-\infty}^{\infty}d\varepsilon_2\frac{\partial n}{\partial\varepsilon_1}\frac{\partial n}{\partial\varepsilon_2}K(\varepsilon_1,\varepsilon_2;\omega_1,\omega_2), \tag{48}$$

where $n=n(\varepsilon,T)$ is a Fermi distribution, and $K(\varepsilon_1,\varepsilon_2;\omega_1,\omega_2)$ is the irreducible average of two current loops. At times for which $\langle\sigma(t)\rangle$ is determined by expression (5), the quantity $K(\varepsilon_1,\varepsilon_2;\omega_1,\omega_2)$ is determined by the diagrams in Fig. 5. The distinction from the $T=0$ case is that ω_1 is replaced by $\omega_1+\Delta\varepsilon$ in the diffusion poles, while ω_2 is replaced by $\omega_2-\Delta\varepsilon$, where $\Delta\varepsilon=\varepsilon_1-\varepsilon_2$. Calculations yield

$$K_T(t_1,\ t_2)=K_0(t_1+t_2)R^2(t_1-t_2), \tag{49}$$

where K_0 is given by expression (46) with $k=2$, and the function

$$R(t)=\int_{-\infty}^{\infty}d\varepsilon\frac{\partial n}{\partial\varepsilon}\cos(\varepsilon t)=\frac{\pi Tt/\hbar}{\mathrm{sh}(\pi Tt/\hbar)} \tag{50}$$

falls off exponentially for $t>\hbar/T$.

Expression (49) continues to hold at long times, where K_0 is determined by asymptotic expression (45), as can be shown by modifying the expanded nonlinear σ model (Secs. 3 and 4) for the calculation of the correlation function $K(\varepsilon;\omega)$ in (48). To calculate this correlation function, we can use expression (40), replacing the matrix $\omega\Lambda$ [see (41)] in the functional $\mathcal{F}$ by the matrix $\hat{\varepsilon}+\omega\Lambda$, where $\hat{\varepsilon}$ is a matrix which is diagonal in the indices i,j and which is a unit matrix with respect to the other indices. As a result, $\omega_{1,2}$ is replaced by $\omega_{1,2}\pm\Delta\varepsilon$ in expansion (42) ($k=2$). When we then use the growth law (43) for the coefficients of this expansion and carry out calculations similar to those described in Secs. 3 and 4, we in fact find expression (49).

The exponential decay of the correlation functions (49) for $|t_1-t_2|>\hbar/T$ evidently means that the response function $\sigma(t)$ is jagged in a specific sample. In other words, there are aperiodic oscillations in this function which are reproducible for a given sample, with an average period on the order of $\hbar/T$.

The jaggedness of the response function means that the hypothesis of an ergodic nature holds for it: Taking an average of $\sigma(t)$ over a time interval $\Delta t\gg\hbar/T$ (but $\Delta t\ll t$) is equivalent to taking an average over an ensemble of samples. For proof it is sufficient to consider the quantity

$$\overline{K(t,t)_{\Delta t}}=\langle\overline{(\sigma(t)_{\Delta t}-\langle\sigma(t)\rangle)^2}\rangle$$

$$= \frac{1}{(\Delta t)^2} \int_{t-\Delta t/2}^{t+\Delta t/2} \int K_T(t_1, t_2)\, dt_1\, dt_2, \qquad (51)$$

where the superior bar means an average over the interval Δt:

$$\overline{\sigma(t)}_{\Delta t} \equiv \frac{1}{\Delta t} \int_{t-\Delta t/2}^{t+\Delta t/2} \sigma(t')\, dt'. \qquad (52)$$

Substituting (49) and (50) into (51), we find

$$\overline{K(t,t)}_{\Delta t} \sim \frac{\hbar}{T\Delta t} K_0(2t), \qquad (53)$$

where $K_0(2t)$ is the variance of the fluctuations in $\sigma(t)$ at $T=0$, which is found from (45) or (46) in the case $t_1 \approx t_2 = t$ ($k=2$). This result means that the variance of the response function averaged over the time interval Δt decreases by a factor of $(T\Delta t/\hbar)^{1/2}$.

This suppression of the fluctuations in $\sigma(t)$ has the consequence that even in the case under consideration here, $L < (D\tau_{\varphi 0})^{1/2}$, there is an interval of times in which it is possible to observe a log-normal asymptotic behavior in a specific sample. A direct comparison of (53) and (7) shows that the fluctuations are small for $t \lesssim t_0 (L/l)^{\beta}$, where $\beta \gtrsim (4d\varepsilon)^{1/2}$. This interval of times arises, however, only in the case $d = 2+\varepsilon > 2$ near the Anderson transition. These limitations on the range of applicability of the log-normal asymptotic behavior are removed when we take account of inelastic processes in the volume, to which we now turn.

6. RESPONSE FUNCTION WITH INELASTIC PROCESSES

How do the relaxation processes unfold at temperatures $T \gtrsim \hbar/\tau_{\varphi 0}$, where it is necessary to take account of the phase relaxation of the electron wave function during inelastic interactions in the volume? For definiteness, we restrict the analysis to a qualitative description of the electron-phonon interaction, although the arguments presented below remain valid when any type of inelastic interaction is taken into account. Our goal is to show that there exists a wide range of phase relaxation times with a distribution function $f(t_\varphi)$ which has a log-normal asymptotic behavior. A response function found by averaging $\exp(-t/t_\varphi)$ with a weight $f(t_\varphi)$ will then have a log-normal asymptotic behavior, (7), after long times.

The inverse effect of the phonon-electron relaxation is determined by a diagram of the type shown in Fig. 6a. We know quite well that a slight disorder does not affect this quantity. In an ensemble of conductors of mesoscopic dimensions ($L \lesssim L_{\varphi 0} \equiv (D\tau_{\varphi 0})^{1/2}$), however, this quantity (and the reciprocal of the phase relaxation time, τ_φ^{-1}, which is proportional to it) fluctuates from sample to sample in a manner reminiscent of the behavior of the conductivity or the density of electron states.

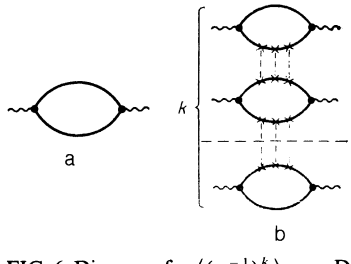

FIG. 6. Diagrams for $\langle(\tau_\varphi^{-1})^k\rangle_c$. a—Diagram for $\langle\tau_\varphi^{-1}\rangle$; b—diagram for the higher-order fluctuation moments $\langle(\tau_\varphi^{-1})^k\rangle_c$ in lowest order in α. At a transition to the next order in α (when yet another interloop diffusion or cooperon is added), the number of diagrams is increased by a factor of k^2.

The distribution function $f(\tau_\varphi)$ can be reconstructed if we know all the fluctuation moments of this quantity. The most substantial contribution to $\langle(\tau_\varphi^{-1})^k\rangle_c$—the kth moment of the mesoscopic fluctuations in τ_φ^{-1}—is described by diagrams of the type shown in Fig. 6b at large values of k. These diagrams look exactly like the diagrams which describe the mesoscopic fluctuations in the static conductivity or state density.[5] The sole distinction is that a vortex in each loop corresponds in this case to a traceless tensor $q_\alpha q_\beta - q^2\delta_{\alpha\beta}d^{-1}$ instead of a vector, for the conductivity, or a scalar, for the state density. This sole distinction is totally irrelevant to an evaluation of diagrams. The reason is that these estimates are based exclusively on a computation of the number of ways in which the diffusions or cooperons can be arranged in each diagram. Such a computation shows that, as in Ref, 5, in the calculation of the higher-order moments we cannot restrict the analysis to low-order perturbation theories in α [see (12)], since a power series in the parameter $n^2\alpha$ arises.

The moments of τ_φ^{-1} are calculated on the basis of the expanded σ model. The calculation is essentially the same as that which yields the fluctuation moments of the conductivity. The additional vortices in this case contain powers of the tensor source $h_{\alpha\beta}$ and have the (symbolic) form $\mathrm{tr}(hQhQ)^k$. Vertices of this type, in low orders (with respect to h), are presented (in a different notation) in Ref. 22. We will omit the procedure for renormalizing the charges for these vortices, since this procedure differs from that presented above (Secs. 3 and 4) only in inconsequential details. As a result we find that, at large values of k, we have

$$\langle(\tau_\varphi^{-1})^k\rangle_c \tau_{\varphi 0}{}^k \sim (l/L)^{2(k-1)} \exp(k^2 u). \qquad (54)$$

This expression is determined by vortices which contain high powers of the tensor source h. There is of course a contribution to $\langle(\tau_\varphi^{-1})^k\rangle_c$ from the multiple differentiation [of the form (40)] of the vortex which contains only the second power of the source. (In lowest-order perturbation theory, this contribution is described by diagrams similar to those in Fig. 5.) This contribution does not contain powers of the small parameter l/L, so it is predominant at small values of k. At large values of k, the contribution (54) dominates.

The distribution function $f(\tau_\varphi)$ is reconstructed from its moments in the same way as for the distribution function of the mesoscopic fluctuations in the conductance and the state density.[5] As a result we find a distribution function with a comparatively sharp Gaussian peak at $\tau_\varphi \approx \tau_{\varphi 0}$ and a log-normal asymptotic behavior at large τ_φ (Fig. 2). The region $\tau_\varphi \sim \tau_{\varphi 0}$ is determined by the contribution of relatively low-order moments, while the asymptotic behavior is determined by the contribution (54), of large-k moments.

This analysis has been carried out for samples of mesoscopic dimensions. It is in this case that we can ignore the higher orders of the electron-phonon interaction, and we can skip the procedure of making τ_φ^{-1} self-consistent. It is physi-

cally clear, however, that in the limit $L \to \infty$ we are interested in fluctuations in τ_φ^{-1} not throughout the volume but in domains with dimensions on the order of $L_{\varphi 0}$. In this case, the log-normal asymptotic behavior of the relaxation current in the sample is found when we average the contributions from all such domains with the distribution function found here. This distribution function essentially describes fluctuations in this local phase relaxation time.

We note in conclusion that the quantity u, which characterizes the log-normal asymptotic expressions in (7) and (38), increases toward the Anderson transition. As u is increased, the log-normal part of the distribution function (Fig. 2) extends to cover nearly the entire fluctuation region, so the transition to the insulating state should also be accompanied by a pronounced slowing of all relaxation processes. As the transition is approached, the distribution function of the static conductivity and the state density behave in a similar way.[5] This result seems quite natural when we recall that in the one-dimensional case, i.e., the purely insulating case, the fluctuations in the resistance[23,24] and (as was recently established) those in the state density[5,25] are described by log-normal distributions. The transition to an insulating state should accordingly be accompanied by a transition from a normal distribution in the metal to a log-normal distribution in the insulator. The asymptotic form of the distribution is log-normal even in a metal, reflecting the contributions of atypical realizations of the random potential which are insensitive to the metal-insulator transition.

We are deeply grateful to A. G. Aronov, P. B. Vigman, V. P. Prigodin, D. E. Khmel'nitskiĭ, and V. I. Yudson for useful discussions.

[1)]The frequency dependence in this, as in any other, specific diagram can of course be calculated exactly, without an expansion in ω. However, a direct summation of all of the important diagrams cannot be carried out either in an expansion in ω or without such an expansion. A representation of the diagram results as a power series in ω is convenient for making a comparison with the results of an analysis of the nonlinear σ model (Sec. 3), where a different representation of the frequency dependence would not be possible.

[2)]We are setting $\hbar = 1$ in all of the intermediate equations; we restore the correct dimensionality in the estimates and the final expressions.

[3)]In this notation, F_2^0 is the same as the functional (15a), and F_0^1 is the same as functional (15b), of the ordinary σ model.

[4)]The complete set of important operators in the renormalization (26) includes all the vertices which are generated during renormalization-group transformations. These vertices are found from (26) by carrying out a partition into all possible products of matrix traces,[5,9] so that the number of coupled renormalization-group equations, which is equal to the number of these vertices, is determined by the number of partitions of the natural number $N + 2$ into sums of natural numbers. Only the contribution of the maximum eigenvalue of this system of equations is incorporated in (27).

[5)]All vertices which are generated during the renormalization of vertices (32) contribute to this sum. They contain the same number of derivatives as in (32), but their tensor structure is arbitrary, and the integrand is partitioned into the product of all possible matrix traces, as in the case of the renormalization of gradient-free vertices of high order in $\omega\tau$ (Refs. 9 and 5).

[1]P. A. Lee and T. V. Ramakrishnan, Rev. Mod. Phys. **57**, 287 (1985).
[2]B. L. Altshuler, A. G. Aronov, D. E. Khmelnitskiĭ, and A. I. Larkin, in *Quantum Theory of Solids* (ed. I. M. Lifshits), *Advances in Science and Technology in the USSR*, Mir, Moscow, 1982, p. 130.
[3]E. Abrahams, P. W. Anderson, D. C. Licciardello, and T. V. Ramakrishnan, Phys. Rev. Lett. **42**, 673 (1979).
[4]D. J. Thouless, Phys. Rev. Lett. **39**, 1167 (1977).
[5]B. L. Al'tshuler, V. E. Kravtsov, and I. V. Lerner, Zh. Eksp. Teor. Fiz. **91**, 2276 (1986) [Sov. Phys. JETP **64**, 1352 (1986)]; Pis'ma Zh. Eksp. Teor. Fiz. **43**, 342 (1986) [JETP Lett. **43**, 441 (1986)].
[6]B. L.Al'tshuler, Pis'ma Zh. Eksp. Teor. Fiz. **41**, 530 (1985) [JETP Lett. **41**, 648 (1985)].
[7]P. A. Lee and A. D. Stone, Phys. Rev. Lett. **55**, 1622 (1985).
[8]B. L. Al'tshuler and B. I. Shklovskiĭ, Zh. Eksp. Teor. Fiz. **91**, 220 (1986) [Sov. Phys. JETP **64**, 127 (1986)].
[9]V. E. Kravtsov and I. V. Lerner, Zh. Eksp. Teor. Fiz. **88**, 1281 (1985) [Sov. Phys. JETP **61**, 758 (1985)].
[10]L. P.Gor'kov, A. I. Larkin, and D. E. Khmel'nitskiĭ, Pis'ma Zh. Eksp. Teor. Fiz. **30**, 248 (1979) [JETP Lett. **30**, 228 (1979)].
[11]F. Wegner, Z. Phys. **B35**, 207 (1979).
[12]L. Schäfer and F. Wegner, Z. Phys. **B38**, 113 (1980).
[13]K. B. Efetov, A. I. Larkin, and D. E. Khmel'nitskiĭ, Zh. Eksp. Teor. Fiz. **79**, 1120 (1980) [Sov. Phys. JETP **52**, 568 (1980)].
[14]A. Houghton, A. Jevicki, D. Konway, and A. M. M. Pruisken, Phys. Rev. Lett. **45**, 394 (1980).
[15]S. Hikami, Phys. Rev. **B24**, 2671 (1981).
[16]A. M. M. Pruiskien and L. Schäfer, Nucl. Phys. **B200**, 20 (1982).
[17]F. Wegner, Z. Phys. **B36**, 209 (1980).
[18]B. L. Al'tshuler, V. E. Kravtsov, and I. V. Lerner, Pis'ma Zh. Eksp. Teor. Fiz. **45**, 160 (1987) [JETP Lett. **45**, 199 (1987)].
[19]V. E. Kravtsov and I. V. Lerner, Fiz. Tverd. Tela (Leningrad) **29**, 456 (1987) [Sov. Phys. Solid State **29**, 259 (1987)].
[20]V. K. Dugaev and D. E. Khmel'nitskiĭ, Zh. Eksp. Teor. Fiz. **90**, 1871 (1986) [Sov. Phys. JETP **63**, 1097 (1986)].
[21]A. M. M. Pruisken, Columbia University Preprint, CU-TP-352, 1986.
[22]C. Castellani and G. Kotliar, Phys. Rev. **34**, 9012 (1986).
[23]V. I. Mel'nikov, Fiz. Tverd. Tela (Leningrad) **23**, 782 (1981) [Sov. Phys. Solid State **23**, 444 (1981)].
[24]A. A. Abrikosov, Solid State Commun. **37**, 997 (1981).
[25]B. L. Al'tshuler and V. N. Prigodin, Pis'ma Zh. Eksp. Teor. Fiz. **45**, 538 (1987) [JETP Lett. **45**, 687 (1987)].
[26]V. E. Kravtsov, I. V. Lerner, and V. I. Yudson, Zh. Eksp. Teor. Fiz. **94**, 7 (1988) [Sov. Phys. JETP **67**, (1988)].

Translated by Dave Parsons